Computer-aided Ionic Liquids Design for Separation Processes

Peng, Daili

DOI:
10.33612/diss.168550903

Chapter 3

Computer-aided ionic liquids design and experimental validation for benzene-cyclohexane separation

Abstract

In order to design ionic liquid (IL) solvents for the extractive separation of benzene and cyclohexane from their mixture at 298.15 K, a computer-aided ionic liquid design (CAILD) method is presented. The UNIFAC-IL model is used to calculate the thermodynamic properties while semi-empirical models are employed to predict the physical properties. A mixed-integer nonlinear programming (MINLP) problem is formulated and the top five IL solvents are identified by the BONMIN algorithm. One of the designed ILs [COC_2MIM][Tf_2N] (1-(2-methoxyethyl)-3-methylimidazolium bis(trifluoromethylsulfonyl)imide) is selected to perform the liquid-liquid extraction (LLE) experiment to validate the presented CAILD method. It turns out that [COC_2MIM][Tf_2N] is a promising IL solvent for the extractive separation of benzene and cyclohexane with a distribution ratio higher than 1 and a selectivity higher than 15 at low concentrations of benzene in the raffinate phase. Moreover, the designed ILs are ether-functionalized ILs, which tend to have very favorable physical properties, which in turn makes them potential alternative solvents for this extraction process.

This chapter is based on D. Peng, D. P. Horvat, and F. Picchioni, Computer-aided ionic liquids design and experimental validation for benzene-cyclohexane separation, *Ind. Eng. Chem. Res.* **2021**, 60, 13, 4951-4961.

1. Introduction

Cyclohexane is an important industrial chemical that can be produced by the catalytic hydrogenation of benzene. In order to obtain pure cyclohexane, the unreacted benzene needs to be removed from the product stream with an economically viable process[1]. Due to their close boiling points ($\Delta T_b = 0.6$ ℃ at 1 atm), approximately equal molecular volumes, and the presence of a binary azeotrope, traditional distillation is impractical for the separation of benzene and cyclohexane. Liquid-liquid extraction units, because of the relatively low energy consumption, are most widely used especially for the separation of such mixtures with low aromatic (i.e. benzene) content. The main solvents reported for aliphatic-aromatic liquid-liquid extraction, which have also been used in industrial separation, are organic solvents such as sulfolane. In current processes, the organic solvent is usually withdrawn from the top of the regenerator as a vapor stream and then returned to the bottom of the extractor as a liquid stream. The vaporization of the solvent demands high regeneration costs[2]. Moreover, the organic solvents pose environmental threats because they are generally toxic, volatile, and flammable. Hence, it is important to seek economic and environmentally friendly alternative solvents for the purpose of sustainable development and clean processes of chemical engineering.

Ionic liquids (ILs) are widely considered as innovative "green" solvents in separation processes[3-9] because of their very attractive physical properties, such as negligible vapor pressure, high thermal and chemical stability, wide liquid-phase range, and low toxicity. In addition, since their thermophysical properties can be tailored by judicious selection of cations, anions, and substituents, ILs are always referred as "designer solvent". However, the huge number of possible cation and anion combinations makes it very challenging to select a suitable IL for a specific separation task[10]. Obviously, experimental trial and error approaches are not practical to screen ionic liquid solvents as they are time and labor intensive, and strongly dependent on personal experience. Furthermore, the screened ILs are always not optimal because it

is not realistic to test all possible combinations of the cation and the anion. Therefore, it is necessary to use an efficient and reliable tool to guide the selection of ILs for specific usage.

Computer-aided molecular design (CAMD) is a technique that has been widely used to design and develop chemical products, such as pharmaceutical drugs, solvents, and other functional fine chemicals. In the past few years, CAMD has been extended to the design of IL solvents[11-15], namely computer-aided IL design (CAILD). The key to the successful development and use of CAILD methods is the availability of predictive models for the properties of interest. For the extraction process, the prediction of the activity coefficient of different solutes in ILs is crucial, and a variety of models have been developed. The classical activity coefficient models, such as NRTL and UNIQUAC, and models from statistical associating fluid theory such as PC-SAFT[16], have been applied for predicting the phase behaviors of IL-containing systems. To be able to make accurate predictions towards the thermodynamic properties, these models need a number of molecule-specific and mixing parameters. In contrast, as a theoretical hybrid approach combining principles of quantum chemistry and molecular thermodynamics, the conductor-like screening-based (COSMO-based) model such as COSMO-RS[17] and COSMO-SAC[18] have been demonstrated to be powerful tools for calculating thermodynamic properties of the activity coefficients of different solutes in ILs and phase equilibria of IL-involved systems. Because of the lack of experimental data for ILs, many researchers[19-25] make use of COSMO methods for *a priori* selection of IL solvents in various separation problems as this only needs the molecular information, i.e. surface screening charge density and cavity volumes. However, the models mentioned above require molecular information rather than group parameters and thus are not suited for CAILD. These models can be used to screen IL rather than directly design IL solvents, unless the group contribution method is applied to the calculation of the molecular parameters.

Compared to other models, the UNIFAC (universal quasichemical functional-group activity coefficients) model is based on the chemical groups information and widely used in separation science because its formulation is simple and can be directly incorporated into widely used software, such as ASPEN PLUS and PROII, in order to establish equilibrium stage (EQ) and nonequilibrium stage (NEQ) models for design and simulation[26]. Moreover, the group parameters are all regressed from the experimental data which makes the prediction more accurate. Considering all these advantages, the UNIFAC model has been used in many CAILD problems such as CO_2 absorption[27], extraction[28], and extractive distillation[29]. It is worth mentioning that, in most CAILD works only purely simulated data are presented, if the corresponding experiments are available it will provide direct evidence to the design results[30].

In this work, a CAILD framework is presented (Fig. 1) for the design of suitable IL solvents for the extraction of benzene from cyclohexane. At first, with the group contribution (GC) models for the IL physical properties, the UNIFAC-IL model for thermodynamic property prediction and structural constraints, a mixed-integer nonlinear programming (MINLP) problem is formulated. Then, the MINLP problem is solved by the BONMIN algorithm, and the top five ILs are thus predicted. After that, in order to validate the proposed CAILD method, one of the designed IL is selected to perform the liquid-liquid extraction (LLE) experiment. Finally, the performance of the designed IL solvent for the extractive separation of benzene and cyclohexane is compared with that of the organic solvents, ILs, and deep eutectic solvents (DESs) in the literature.

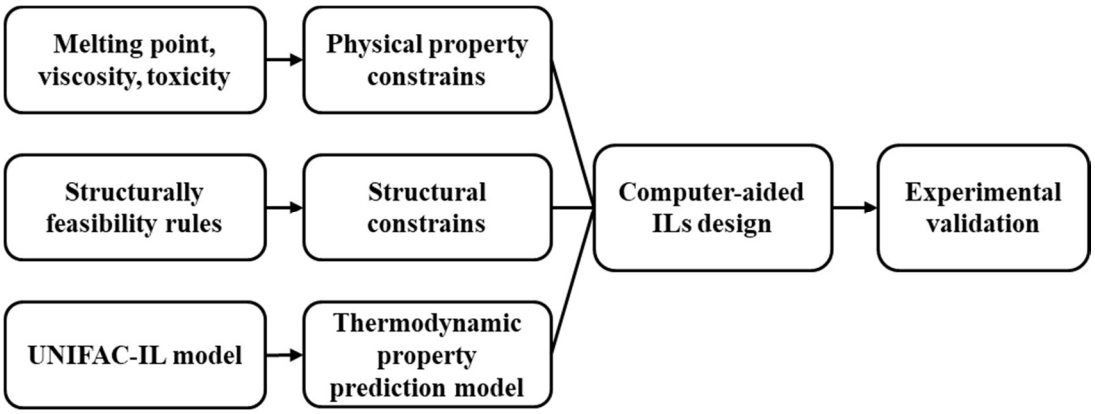

Fig. 1. Proposed CAILD method.

2. CAILD

2.1. UNIFAC-IL model

For the selection of appropriate ionic liquid solvents, the infinite dilution solute distribution coefficient and selectivity provide a useful index[31], which are defined as

$$\beta_1^{\infty} = \frac{1}{\gamma_1^{\infty}} \tag{1}$$

$$S_{12}^{\infty} = \frac{\gamma_2^{\infty}}{\gamma_1^{\infty}} \tag{2}$$

where γ_1^{∞} and γ_2^{∞} represent the activity coefficients of benzene and cyclohexane in the IL solvent, respectively; β_1^{∞} stands for the solute distribution coefficient of benzene; S_{12}^{∞} denotes the separation selectivity.

In order to predict the infinite dilution activity coefficient of the IL-contained system, the UNIFAC-IL model proposed by Lei et al.[26,32] is used. The UNIFAC-IL model is the extension of the original UNIFAC model which was proposed by Fredenslund et al. in 1975[33]. The activity coefficient is expressed as functions of composition and temperature and can be calculated by adding the combinatorial and residual contribution (Eq. 3).

$$\ln \gamma_i = \ln \gamma_i^C + \ln \gamma_i^R \tag{3}$$

In Eq.3, the combinatorial contribution, i.e. $\ln \gamma_i^C$, is essentially due to differences in size and shape of the molecules, and a residual contribution, $\ln \gamma_i^R$, is connected to

energetic interactions. The detailed calculation procedure of $\ln \gamma_i^C$ and $\ln \gamma_i^R$ is described in chapter 1.

To apply the UNIFAC model, the IL must be decomposed into separate functional groups. In the UNIFAC-IL model, as shown in Fig. 2, the IL is divided into two parts, the skeletons of cation and anion are treated as one part (main group) since the ionic pair has a strong electrostatic interaction, and the substituents in the cation is treated as the other part. With this decomposition method, ILs are decomposed into electrically neutral groups, and the additional terms accounting for long electrostatic contributions can be avoided. The UNIFAC-IL method is capable of quantitative prediction of the thermodynamic property of the benzene-cyclohexane-IL system. The ARDs (average related deviations) between the experimental and calculated distribution ratio and selectivity are 10.34 and 28.68, respectively[32].

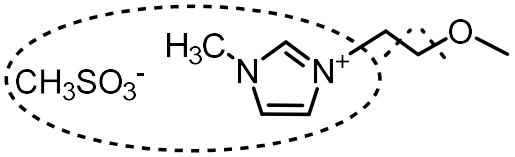

Fig. 2. Group segmentation exemplified for [COC_2IM][CH_3SO_3] (1-(2-methoxyethyl)imidazolium methanesulfonate).

2.2. Design problem formulation

The CAILD problem consists of two parts, i.e. objective function (Eq. 4) and thermophysical constraints (Eqs. 5-6). The objective function stands for the goal of CAILD while the constraints guarantee the designed ILs meet the desired requirements.

$$\max.\ or\ \min.\ OF = f(v) \tag{4}$$

s.t.

$$h(v) \leq 0 \tag{5}$$

$$g(v) \leq 0 \tag{6}$$

where $[v_1,\ v_2,\ \dots,\ v_k]$ is a vector containing the frequency of the candidate groups; $f(v)$ is the objective function; $h(v)$ and $g(v)$ are the structural constraints and physical property constraints, respectively.

In the liquid-liquid extraction process, the solute distribution coefficient indicates the solvent usage, whereas selectivity mainly evaluates the product purity. Ideally, the designed IL solvent should display a high distribution coefficient (Eq. 1) and selectivity (Eq. 2) at the same time, however, the distribution coefficient is mostly inversely related to the selectivity[34]. Thus, in order to evaluate the overall performance of IL solvents, the objective function is set to PI^{∞} (performance index, Eq. 7), which is defined as the product of the selectivity and the solute distribution coefficient at infinite dilution[35].

$$PI^{\infty} = \beta_1^{\infty} \times S_{12}^{\infty} \tag{7}$$

The structural constraints are applied to ensure only structurally feasible ILs are designed from the collection of building blocks, and some rules are used for this purpose including octet rule, bonding rule, and complexity rules. Eq. (8) is used to guarantee the designed ILs only include one anion and one cation. Eq. (9) is the octet rule which can avoid free bonds in ILs. The number of each substituent group is limited by Eq. (10), and the complexity of the IL structure is confined by Eq. (11). In this work, LB and UB are set to 1 and 7, respectively. Besides, the total number of substituents on cation skeletons, except CH_2 and CH_3, is set to less than or equal to 1. This constraint can be relaxed if more functional groups are required in the CAILD.

$$\sum_{i \in main} v_i = 1 \tag{8}$$

$$\sum_{i \in main,Sub} (2 - e_i) v_i - 2 = 0 \tag{9}$$

$$LB \leq v \leq UB \tag{10}$$

$$\sum_{i \in sub^*} v_i \leq 1 \tag{11}$$

where $main$ is the set of the combination of cation skeletons and anion; e_i is group valence of group i; LB and UB are the lower and upper bound, respectively; Sub

denotes the set of substituent groups on the cations, while Sub^* represents the subset of functional substituent groups except for CH_2 and CH_3.

In order to design IL solvents with proper physical properties, the constraint related to the melting point ($T_m < 298.15$ K) and viscosity ($\eta < 100$ cp) are included in the CAILD framework. The prediction of these physical properties is based on two semi-empirical models developed by Lazzús et al.[36,37], and the corresponding parameters are listed in Table S1.

The melting point is calculated as follows:

$$T_m = 288.7 + \sum_{i=1}^{n_g} v_i \Delta t_i \tag{12}$$

where Δt_i is the contribution of the group i to the melting point.

The viscosity of ILs is calculated by:

$$\ln \eta = 6.982 + \sum_{i=1}^{n_g} v_i a_i + \frac{\sum_{i=1}^{n_g} v_i b_i}{T} \tag{13}$$

where a_i and b_i are the contribution parameters of group i to the viscosity of ILs.

Moreover, due to the high solubility of many ILs in water, they can be released into the environment through wastewater, several studies showed that ILs have hazardous potential to the ecosystem[38,39]. Therefore, the toxicity of ILs should also be treated as a constraint when designing ILs. In this work, the half-maximal effective concentration (EC50) of the biological endpoints of Leukemia Rat Cell Line (IPC-81) is used to evaluate the toxicity of ILs. The EC50 of IPC-81 is estimated by a GC-based method[40]. According to the UFT research center (center for environmental research and sustainable technology), the logEC50 of ILs should higher than 2 to ensure they do not possess high toxicity.

With the objective function and constraints mentioned above, the CAILD problem for the extractive separation of benzene and cyclohexane at room temperature can be described as an MINLP problem:

$$\max. PI^{\infty} = f(v) \quad (14)$$

s.t.

Eqs. (8) - (11)

$$T_m < 298.15 \text{ K} \quad (15)$$

$$\eta < 100 \text{ cp} \quad (16)$$

$$\log EC50 > 2 \quad (17)$$

It is worth mentioning that not all the groups in the UNIFAC-IL model have the parameters for the calculation of melting point and viscosity, thus these groups are discarded during the CAILD.

2.3. Solving the MINLP problem

Although the presented CAILD problem can be solved by the generate-and-test method[41,42], this is very time-consuming, and problems with a large design space are not solved efficiently with this approach[43]. Considering the large amount of ILs, it is necessary to solve this problem through a more efficient algorithm. In this work, the presented MINLP problem is solved by Matlab (R2018b) using the BONMIN algorithm[44] in an OPTI Toolbox27.

Due to the lack of experimental data, the UNIFAC-IL group interaction parameters are not available for every group pairs which makes solving this problem by the BONMIN algorithm very challenging. To avoid this problem and simplify the solving procedure the design space is devised into several subsets following the steps:

(1) Firstly, the UNIFAC-IL parameters matrix is generated and it only includes IL main groups having the interaction parameters with the groups in cyclohexane and benzene, i.e. CH_2 and ACH.

(2) Then, the main groups without the parameters for the calculation of physical properties are discarded.

(3) Finally, the design space for every main group is assigned according to the availability of the UNIFAC-IL parameters (Fig. 3). For example, the design space (marked as red) for main group [MIM][BF_4] is {1-7, 9, 11}, for [MIM][TFA] is {1-7}, and for [P][CH_3SO_4] is {1-3}, respectively.

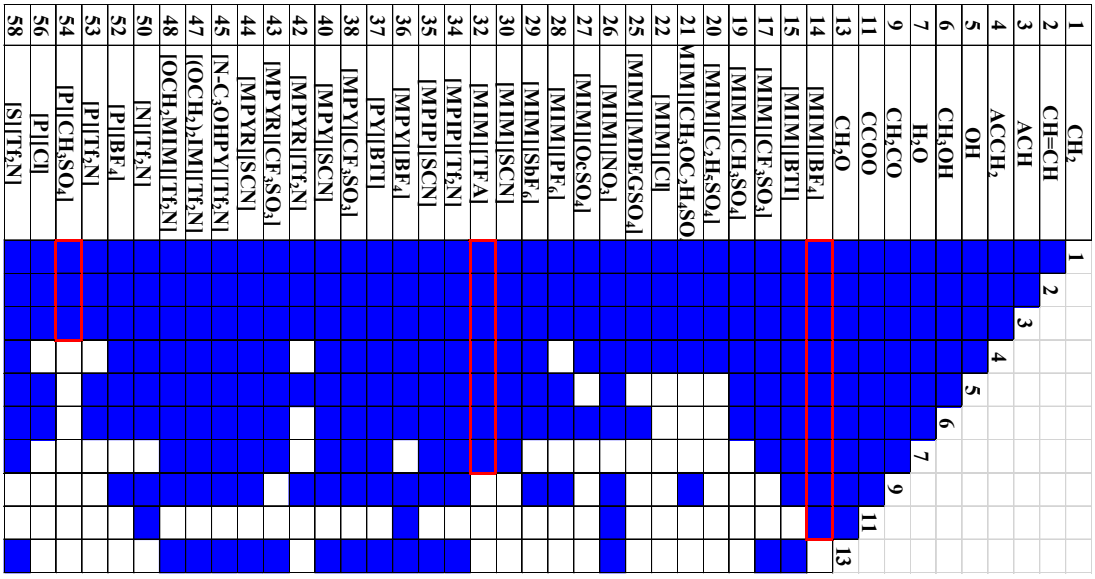

Fig. 3. Design space for the proposed CAILD.

After generating the design space for every main group, the design procedure will start using the BONMIN algorithm. In order to find the global optimal solution, several conventional and functionalized ILs are set as the initial value. Moreover, after the optimal structure of IL is generated, this solution will be continuously removed from the design space using the integer cut[46] before starting the next optimization. Eventually, the top 5 ILs with the desired thermophysical properties can be output.

3. Experimental

3.1. Materials

The ionic liquid [COC_2MIM][Tf_2N] (1-(2-methoxyethyl)-3-methylimidazolium bis(trifluoromethylsulfonyl)imide) with purities > 98% is purchased from IoLiTec, and the structure is shown in Fig. 4. Benzene and cyclohexane are purchased from TCI Europe N.V. with purities > 99.5% and used as received.

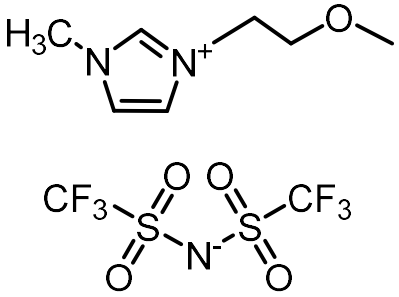

Fig. 4. Structure of the designed IL [COC_2MIM][Tf_2N].

3.2. Liquid-liquid extraction

A mixture containing 5 wt% benzene, 45 wt% cyclohexane, and 50 wt% ionic liquid is weighted and added to a 10 mL round bottom flask with a cap covered in parafilm in order to avoid chemical loss. The measurements are performed in grams and the total composition is set to 4 g using an analytical balance (Mettler AE200) with the readability of $\pm$0.0001 g. The same procedure is carried for higher concentrations of benzene (i.e. 10 wt%, 15 wt%, 20 wt%, 25 wt%, and 30 wt%) in the feed while keeping 50 wt% of the ionic liquid. The liquid-liquid extraction experiments are carried out at isothermal conditions at 298.15 K ($\pm$0.1 K) controlled by the water bath equipped with the IKA ETS-D5 contact thermometer. The flask is put into the water bath stirred for 6 h at 500 rpm and left to settle 12 h to reach complete thermodynamic equilibrium.

3.3. Determination of the ternary molar composition

Samples are carefully taken with syringes from the cyclohexane-rich layer and IL-rich layer and then determined by gas chromatography (GC) and nuclear magnetic resonance (NMR), respectively. The samples from the cyclohexane-rich layer are firstly confirmed to be totally free of ILs by ^{1}H NMR analysis (Varian Mercury Plus-400). The GC equipment used is the Thermo Finnigan Trace GC Ultra with a flame ionization detector (FID) and a Restek Stabilwax-DA column (30 m × 0.32 mm × 1 μm). The IL-rich layer could not be subjected to GC analysis due to the negligible vapor pressure, therefore, the samples are prepared by dissolving a drop in $\pm$0.7 mL of deuterated methanol placed inside an NMR tube and analyzed by the NMR 400 MHz spectrometer. The average uncertainty on the mole fraction of the GC and ^{1}H NMR analysis is estimated to be less than 0.003. The detailed description of the analysis procedures can be found elsewhere[10,34].

3.4. Evaluation of solvent extraction performance

The molar-based distribution coefficient (β) of benzene and the solvent selectivity (S) of IL is used to evaluate the performance of the IL solvents for the liquid-liquid extraction process

$$\beta_1 = \frac{x_1^E}{x_1^R} \tag{18}$$

$$S_{12} = \left(\frac{x_1^E}{x_1^R}\right) \Big/ \left(\frac{x_2^E}{x_2^R}\right) \tag{19}$$

where x_1 and x_2 are the concentrations of benzene and cyclohexane, respectively. The superscripts E and R represent the extract and raffinate phase, respectively.

3.5. Consistency tests

In order to test the consistency of the experimental results, the Hand[47] and Othmer-Tobias[48] correlations are conducted using the following equations.

$$\ln\left(\frac{x_1^R}{x_2^R}\right) = a + b\ln\left(\frac{x_1^E}{x_3^E}\right) \quad (20)$$

$$\ln\left(\frac{1-w_2^R}{w_2^R}\right) = c + d\ln\left(\frac{1-w_3^E}{w_3^E}\right) \quad (21)$$

where x_3 and w_3 stand the mole and weight concentrations of IL, respectively. w_2 represents the weight concentrations of cyclohexane. The parameters *a*, *b*, *c*, and *d* are fitted using the experimental data. The linearity of the results (i.e. the value of R^2 close to 1) indicates the consistency for the ternary liquid-liquid extraction tie lines

4. Results and discussions

4.1. CAILD results

The top five IL solvents designed by the presented CAILD method are listed in Table 1 together with their predicted separation performance and physical properties. It can be seen that the designed ILs all have the same main group i.e. [MIM][Tf_2N]. This is consistent with the results from the COSMO-RS screening method[34] where [EMIM][Tf_2N] tends to have a very high PI^{∞}. Although UNIFAC-IL can give quantitative prediction, an experimental validation based on the design results is necessary. In this work, [COC_2MIM][Tf_2N] is chosen to perform the liquid-liquid extraction experiment since it is the only one commercially available among the five designed ILs with predicted optimal performance.

Table 1. CAILD results for the extractive separation of benzene from cyclohexane.

ILs	PI^{∞}	S^{∞}	β^{∞}	η (cP)	T_m (K)	logEC50
[COCMIM][Tf_2N]	66.45	30.44	2.18	35.54	279.06	3.34
[COCIM][Tf_2N]	62.74	29.48	2.13	25.61	262.47	3.39
[COC_2MIM][Tf_2N]	51.94	23.39	2.22	41.47	275.31	3.34
[COC_2IM][Tf_2N]	48.26	22.23	2.17	29.89	258.71	3.38
[COC_3MIM][Tf_2N]	42.48	18.67	2.28	48.40	271.55	3.23

4.2. Liquid-liquid extraction data

The liquid-liquid extraction diagrams at 298.15 K for the ternary system of [COC_2MIM][Tf_2N] + benzene + cyclohexane are displayed in Fig. 5. The molar compositions of the tie-lines are tabulated in Table 2. No ILs are detected in the raffinate phase which means the solvent cross-contamination could be avoided, and it can significantly simplify the liquid-liquid extraction process. Moreover, the concentration of cyclohexane in the extract phase is quite low, which implies that the IL solvent can be easily regenerated. The value of parameters for the consistency tests are listed in Table 3, the fact that the R^2 for both correlations close to 1 suggests a relevant consistency of the experimental data.

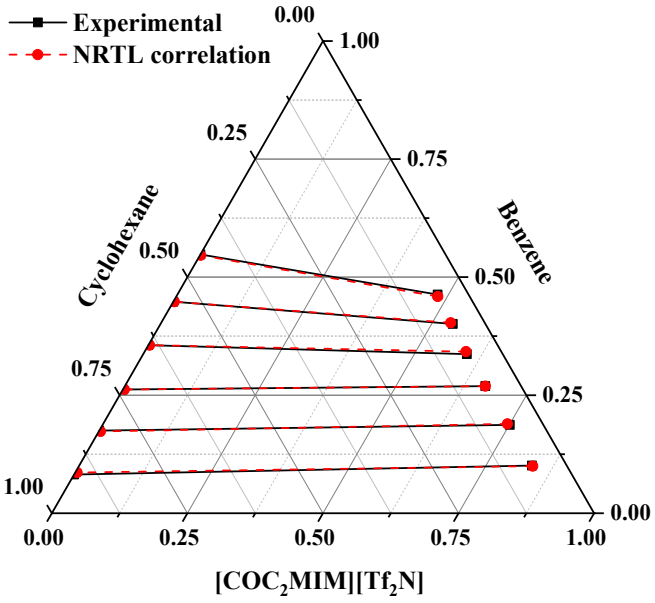

Fig. 5. Tie-lines for the ternary mixture benzene + cyclohexane + [COC_2MIM][Tf_2N] at 298.15 K.

Table 2. Molar composition of the tie-lines with the distribution ratio and selectivity data for (1) benzene + (2) cyclohexane + (3) [COC_2MIM][Tf_2N] at 298.15 K.

Cyclohexane-rich layer		Ionic liquid-rich layer			β	S
x_1	x_2	x_1	x_2	x_3		
0.082	0.918	0.101	0.064	0.835	1.232	17.667
0.175	0.825	0.187	0.062	0.751	1.069	14.219
0.262	0.738	0.269	0.066	0.665	1.027	11.481
0.356	0.644	0.337	0.066	0.597	0.947	9.237
0.448	0.552	0.401	0.060	0.539	0.895	8.235
0.548	0.452	0.463	0.057	0.480	0.845	6.700

Table 3. Parameters of Hand and Othmer-Tobias correlation for (1) benzene + (2) cyclohexane + (3) [COC_2MIM][Tf_2N].

HAND			Othmer-Tobias		
a	b	R^2	c	d	R^2
0.1593	1.2386	0.9966	2.5100	1.5200	0.9976

4.3. NRTL model correlation and validation

The NRTL model[49] is used to correlate the experimental data of the liquid-liquid extraction, the activity coefficient for the component i is given by

$$\ln \gamma_i = \frac{\sum_j \tau_{ji} x_j G_{ji}}{\sum_k x_k G_{ki}} + \sum_j \frac{x_j G_{ij}}{\sum_k x_k G_{kj}} \left(\tau_{ij} - \frac{\sum_m \tau_{mj} x_m G_{mj}}{\sum_k x_k G_{kj}} \right) \quad (22)$$

$$\tau_{ij} = \frac{\Delta g_{ij}}{RT} \quad (23)$$

$$G_{ij} = \exp\left(-\alpha_{ij} \tau_{ij}\right) \quad (24)$$

where Δg_{ij} is an energy parameter that characterizes the interactions between species i and j, x_i is the mole fraction of component i, α_{ij} is a non-randomness parameter related to the mixture which is set to 0.2, R is the gas constant, and T is the absolute temperature. The model parameters Δg_{ij} are optimized using an objective function that minimizes the overall differences between the experimental and calculated mole fractions of the components in the two liquid phases. The regressed parameters are

listed in Table 4, and the small RMSD (root-mean-square deviation) value of 0.0046 between the experimental and NRTL calculation indicates a high regression quality.

Table 4. NRTL parameters regressed from the experimental LLE data for the ternary systems (1) benzene + (2) cyclohexane + (3) [COC_2MIM][Tf_2N] with RMSD between experimental and calculated results.

	NRTL parameters			RMSD
components *i-j*	$(\Delta g_{ij}/R)$/K	$(\Delta g_{ji}/R)$/K	α_{ij}	
1-2	-288.97	5077.92	0.2	0.0046
1-3	797.76	3843.74	0.2	
2-3	-0.18	-60.86	0.2	

In order to check the consistency of the obtained NRTL parameters, a Matlab toolbox for the topological analysis[50] is used. The results are provided in Fig. S1. According to the miscibility boundary analysis, there is one homogeneous region for binary subsystem (1) benzene - (2) cyclohexane and a single liquid-liquid region for the binary subsystems (1) benzene - (3) IL and (2) cyclohexane - (3) IL. The same conclusion can be drawn from the G^M/RT function obtained for each one of the three binary subsystems using the correlated NRTL parameters. The experimental observation is consistent with the topological analysis, the binary subsystem (1) - (2) is totally miscible while the binary subsystems (1) - (3) and (2) - (3) are partially miscible.

4.4. Comparison of the designed ILs with other solvents

Figs. 6 and 7 compare the distribution ratio of benzene and solvent selectivity among diverse solvents including sulfolane, ILs, and DESs[34,51-57], respectively. Sulfolane is treated as a benchmark to represent the performance of the organic solvents used in the industry. It can be seen that at low concentrations of benzene in the raffinate phase, the distribution ratio and the selectivity of the [COC_2MIM][Tf_2N] are higher than that of sulfolane and DESs, which confirms the suitability of the studied ILs as solvents for the separation of benzene and cyclohexane.

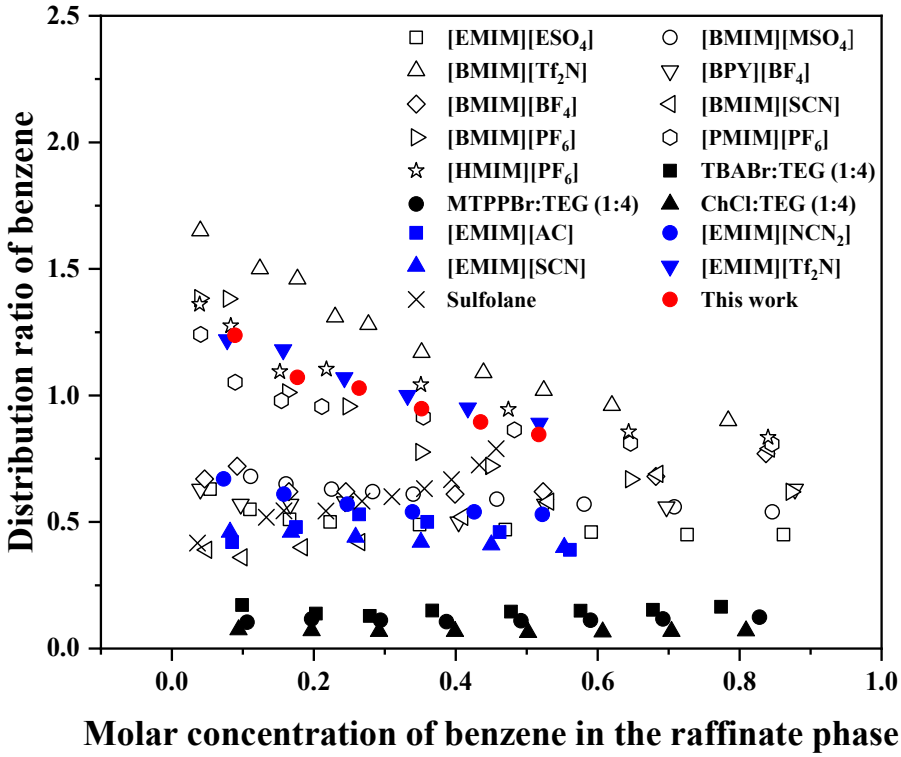

Fig. 6. Ditribution ratio of benzene in sulfolane, ILs, and DESs for the extractive separation of benzene and cyclohexane.

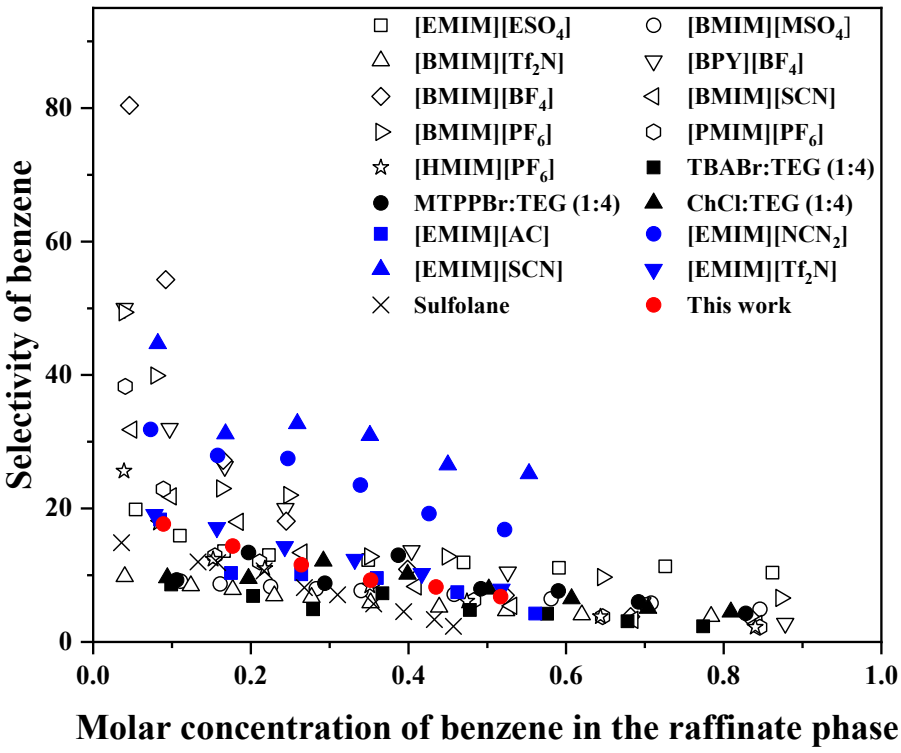

Fig. 7. Selectivity of sulfolane, ILs, and DESs for the extractive separation of benzene and cyclohexane.

Since the distribution coefficient is generally inversely related to the selectivity, many ILs in Figs. 6 and 7 only have an extremely high distribution ratio ([BMIM][Tf_2N]) or selectivity ([BMIM][BF4], [Bpy][BF_4], [EMIM][SCN], and [EMIM][$N(CN)_2$]). In this work, PI^{∞} is used as the objective function to evaluate the overall performance of the extraction process which makes the designed IL [COC_2MIM][Tf_2N] has a high benzene distribution coefficient ($\beta_1 > 1$) and a reasonable solvent selectivity ($S_{12} > 15$) at the low concentrations of benzene in the raffinate phase. This means the liquid-liquid extraction process using [COC_2MIM][Tf_2N] will be very efficient and do not need too many solvents.

Table 5. Comparison of the extraction performance and physical properties among different solvents.

Solvents	$PI_{0.1}$	$\beta_{0.1}$	$S_{0.1}$	T_m (K)	η (cP)	$\log \mathrm{EC50}$[a]
[BMIM][PF_6]	45.22	1.24	36.51	284.10	271.00	3.33
[BMIM][BF_4]	36.06	0.67	53.72	202.15	108.00	3.37
[EMIM][Tf_2N]	22.40	1.21	18.52	274.10	34.40	3.04
[COC_2MIM][Tf_2N]	20.51	1.20	17.10	275.31[a]	41.47[a]	3.34
[EMIM][DCA]	19.96	0.65	30.78	268.30	16.09	3.69
0.5[EMIM][Tf_2N] + 0.5[EMIM][DCA]	19.79	1.00	19.75	< 298.15	-	-
[EMIM][SCN]	18.96	0.46	41.11	266.00	24.50	3.66
[EMIM][ESO4]	9.58	0.57	16.88	236.30	101.55	3.93
[EMIM][AC]	7.14	0.43	16.49	228.15	143.60	3.60
sulfolane	6.25	0.47	13.28	300.75	10.07	-

[a] Calculated values

The performance index of various solvents as well as the distribution and selectivity at $x_2^R = 0.1$ are listed in Table 5. These values are acquired by using the interpolation method towards the distribution ratio or selectivity curve in Figs. 6 and 7. The melting point and viscosity (at 300.75 K for sulfolane and 298.15 K for other solvents) are acquired from literature[58–67] or online database (ChemSpider). It is worth

mentioning that, the experimental viscosity of [COC_2MIM][Tf_2N] is 41.8 cP[68] which is accorded well with the calculated value (41.47 cP) in this work.

It can be seen that the designed IL [COC_2MIM][Tf_2N] ranks in fourth place in the table, it has a much better performance compared to the organic solvents sulfolane. Although [BMIM][PF_6] has the highest $PI_{0.1}$, it is known as a viscous IL[69] with a viscosity of 271 cP. [BMIM][BF_4] also owns a very high $PI_{0.1}$, however, it shows a low distribution ratio (0.67) and relatively high viscosity (108 cP). [COC_2MIM][Tf_2N] and [EMIM][Tf_2N] have close performance and physical properties because of the similar structure. Nevertheless, [EMIM][Tf_2N] owns the lowest $\log EC50$ value (3.04) which means it is the most toxic IL among the ILs in Table 5. The presence of an ether group in [COC_2MIM][Tf_2N] can decrease its lipophilicity which largely weakens the interactions with the lipid component in the cell membrane and significantly reduces its toxicity[70,71]. Therefore, the designed IL [COC_2MIM][Tf_2N] is a very favorable solvent for the separation of benzene/cyclohexane with good extraction ability, proper physical properties, and relatively low toxicity.

It should be noted that the ILs with $[TCM]^-$ anion (e.g., [Mo1,3CN][TCM] and [Mo1,3OH][TCM]) are also reported to be promising solvents for the extractive separation of benzene/cyclohexane[72]. However, the group interaction parameters between the [TCM]-containing groups and "ACH" group are missing in the used UNIFAC-IL model, thus these ILs are not included in the current design space.

5. Conclusions

A CAILD method is presented to design the suitable IL solvents for the extraction of benzene from its mixture with cyclohexane. The design problem is formulated as an MINLP problem and solved by the BONMIN algorithm. The top five IL candidates with the highest PI^{∞} and favorable physical properties are designed. One of the designed ILs, i.e. [COC_2MIM][Tf_2N], is selected for the experimental validation by the liquid-liquid extraction, and the corresponding NRTL parameters are acquired by correlating the experimental data. It turns out that [COC_2MIM][Tf_2N] shows good performance in the extraction of benzene from the benzene-cyclohexane mixture, and the low melting point, viscosity, and toxicity indicating the potential of this IL as an alternative solvent. The experimental results confirmed that the proposed CAILD is a reliable and useful tool to design suitable ILs for the extractive separation of benzene and cyclohexane. It is worth mentioning that the presented CAILD method can be easily modified by updating the thermophysical prediction models or extend to other separation tasks by adjusting the objective function and constraints.

Nomenclature

β_i^∞	distribution coefficient of component *i* at infinite dilution
β_i	distribution coefficient of component *i*
η	viscosity, Pa.S
e_i	valence of group *i*
E	extract phase
LB	lower bound vector
PI^∞	performance index of extraction at infinite dilution
R	raffinate phase
S_{ij}^∞	infinite dilution selectivity of solvent to the component *i* over *j*
S_{ij}	selectivity of solvent to the component *i* over *j*
T_m	melting point, K
UB	upper bound vector
v_i	frequency of group *i*
x_i	composition of component *i* in liquid
γ_i^∞	infinite dilution activity coefficient of component *i*
[EMIM]	1-ethyl-3-methylimidazolium
[BMIM]	1-butyl-3-methylimidazolium
[PMIM]	1-pentyl-3-methylimidazolium
[HMIM]	1-hexyl-3-methylimidazolium
[BPY]	1-butylpyridinium
[COCIM]	1-(2-methoxymethyl)-methylimidazolium
[COC_2MIM]	1-(2-methoxyethyl)-3-methylimidazolium
[COC_2IM]	1-(2-methoxyethyl)-methylimidazolium
[COC_3MIM]	1-(2-methoxypropyl)-3-methylimidazolium
[MSO_4]	methylsulfate
[ESO_4]	ethylsulfate
[Tf_2N]	bis(trifluoromethylsulfonyl)imid
[BF_4]	tetrafluoroborate
[SCN]	thiocyanate
[PF_6]	hexafluorophosphate
[Ac]	acetate

$[N(CN)_2]$	dicyanamide
TBABr	tetrabutylammonium bromide
TEG	triethylene glycol
MTPPBr	methyltriphenylphosphonium bromide
ChCl	choline chloride

Supporting Information

Table S1. Group parameters for the prediction of melting point and viscosity of ILs.

Index	Subgroup	*a*	*b*	Δt_c
1	CH_3	-4.28	769.42	-4.38
2	CH_2	-0.05	60.96	-3.76
3	CH	-1.60	1129.10	13.13
4	C	-4.71	2396.60	76.19
5	CH_2=CH	-7.53	1697.90	-9.96
6	OH	63.43	-19200.00	-14.99
7	CH_3O	-8.56	2050.22	-14.85
8	CH_2O	-4.33	1341.76	-14.23
9	CHO	-5.88	2409.90	2.66
10	[MIM][BF_4]	-12.57	3470.42	61.89
11	[IM][BF_4]	-17.41	4817.00	45.30
12	[MIM][Tf_2N]	0.56	-726.68	8.97
13	[IM][Tf_2N]	-4.28	619.90	-7.62
14	[MIM][CF_3SO_3]	-9.32	2336.15	53.09
15	[IM][CF_3SO_3]	-14.16	3682.73	36.50
16	[MIM][CH_3SO_4]	-11.35	3182.32	33.92
17	[IM][CH_3SO_4]	-16.19	4528.90	17.33
18	[MIM][$C_2H_5SO_4$]	-11.74	3257.02	38.19
19	[IM][$C_2H_5SO_4$]	-16.58	4603.60	21.59
20	[MIM][$CH_3OC_2H_4SO_4$]	-15.50	5008.92	35.74
21	[IM][$CH_3OC_2H_4SO_4$]	-20.35	6355.50	19.15
22	[MIM][Cl]	-12.42	4298.82	97.10

23	[IM][Cl]	-17.27	5645.40	80.50
24	[MIM][$MDEGSO_4$]	-15.50	5008.92	37.57
25	[IM][$MDEGSO_4$]	-20.35	6355.50	20.97
26	[MIM][NO_3]	-18.38	5374.12	55.60
27	[IM][NO_3]	-23.23	6720.70	39.01
28	[MIM][$OcSO_4$]	-12.17	3828.42	63.77
29	[IM][$OcSO_4$]	-17.01	5175.00	47.17
30	[MIM][PF_6]	-13.62	4058.62	81.10
31	[IM][PF_6]	-18.46	5405.20	64.51
32	[MIM][SbF_6]	-7.80	2006.99	0.77
33	[IM][SbF_6]	-12.65	3353.57	-15.83
34	[MIM][SCN]	-11.36	2897.62	20.47
35	[IM][SCN]	-16.20	4244.20	3.87
36	[MIM][TFA]	-10.57	2682.82	-12.63
37	[IM][TFA]	-15.42	4029.40	-29.23
38	[MPIP][Tf_2N]	4.06	-1366.51	13.17
39	[PIP][Tf_2N]	-0.78	-19.93	-3.42
40	[MPIP][SCN]	-7.85	2257.79	24.67
41	[PIP][SCN]	-12.70	3604.37	8.07
42	[MPY][BF_4]	-17.05	4914.02	66.46
43	[PY][BF_4]	-21.90	6260.60	49.87
44	[MPY][BTI]	-3.93	716.92	13.54
45	[PY][BTI]	-8.77	2063.50	-3.05
46	[MPY][CF_3SO_3]	-13.81	3779.75	57.66
47	[PY][CF_3SO_3]	-18.65	5126.33	41.07
48	[MPY][SCN]	-15.84	4341.22	25.04
49	[PY][SCN]	-20.69	5687.80	8.44
50	[MPYR][Tf_2N]	-94.37	27758.42	42.85
51	[PYR][Tf_2N]	-99.22	29105.00	26.26
52	[MPYR][CF_3SO_3]	-104.25	30821.25	86.97
53	[PYR][CF_3SO_3]	-109.10	32167.83	70.38
54	[MPYR][SCN]	-106.29	31382.72	54.35
55	[PYR][SCN]	-111.13	32729.30	37.75

56	[N-C_3OHPY][Tf_2N]	47.94	-14817.63	-40.83
57	[$(OCH_2)_2$IM][Tf_2N]	-3.82	1187.41	-15.10
58	[OCH_2MIM][Tf_2N]	-3.77	615.08	-5.25
59	[OCH_2IM][Tf_2N]	-8.62	1961.66	-21.85
60	[N][Tf_2N]	39.18	-10552.70	74.67
61	[P][BF_4]	8.02	-1465.30	119.11
62	[P][Tf_2N]	21.15	-5662.40	66.19
63	[P][CH_3SO_4]	9.24	-1753.40	91.14
64	[P][Cl]	8.16	-636.90	154.31
65	[S][Tf_2N]	7.97	-1932.93	-5.03

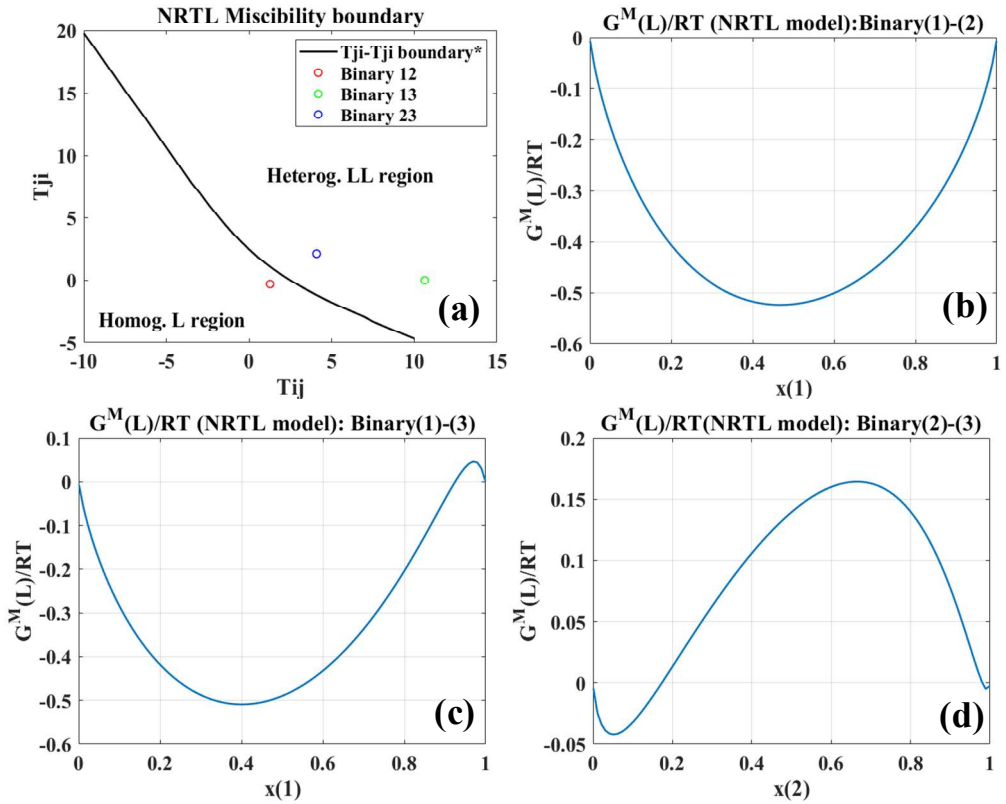

Fig. S1. Results of the topological analysis of NRTL correlation for (1) benzene + (2) cyclohexane + (3) [COC_2MIM][Tf_2N].

References

1 J. G. Villaluenga and A. Tabe-Mohammadi, *J. Memb. Sci.*, 2000, **169**, 159–174.

2 D. F. Schneider, *Chem. Eng. Prog.*, 2004, **100**, 34–39.

3 K. Huang, J.-Y. Zhang, X.-B. Hu and Y.-T. Wu, *Energy Fuels*, 2017, **31**, 14060–14069.

4 Y. Wang, X. Yang, W. Bai, J. Zhang, X. Zhou, X. Guo, J. Peng, J. Qi and Z. Zhu, *ACS Sustain. Chem. Eng.*, 2020, **8**, 4440–4450.

5 Y. Dong, C. Dai and Z. Lei, *Ind. Eng. Chem. Res.*, 2018, **57**, 11167–11177.

6 G. Yu, C. Dai, H. Gao, R. Zhu, X. Du and Z. Lei, *Ind. Eng. Chem. Res.*, 2018, **57**, 12202–12214.

7 K. Huang, X.-M. Zhang, L.-S. Zhou, D.-J. Tao and J.-P. Fan, *Chem. Eng. Sci.*, 2017, **173**, 253–263.

8 P. Wang, D. Xu, P. Yan, J. Gao, L. Zhang and Y. Wang, *J. Mol. Liq.*, 2018, **261**, 89–95.

9 Y. Dong, C. Dai and Z. Lei, *Fuel*, 2018, **216**, 503–512.

10 S. E. McLeese, J. C. Eslick, N. J. Hoffmann, A. M. Scurto and K. V. Camarda, *Comput. Chem. Eng.*, 2010, **34**, 1476–1480.

11 A. T. Karunanithi and A. Mehrkesh, *AIChE J.*, 2013, **59**, 4627–4640.

12 K. Paduszyński, M. Królikowski, M. Zawadzki and P. Orzeł, *ACS Sustain. Chem. Eng.*, 2017, **5**, 9032–9042.

13 D. Peng, J. Zhang, H. Cheng, L. Chen and Z. Qi, *Chem. Eng. Sci.*, 2017, **159**, 58–68.

14 J. Zhang, L. Qin, D. Peng, T. Zhou, H. Cheng, L. Chen and Z. Qi, *Chem. Eng. Sci.*, 2017, **162**, 364–374.

15 T. Zhou, H. Shi, X. Ding and Y. Zhou, *Chem. Eng. Sci.*, 2021, **229**, 116076–116084.

16 K. Paduszyński and U. Domańska, *J. Phys. Chem. B*, 2012, **116**, 5002–5018.

17 A. Klamt and F. Eckert, *Fluid Phase Equilib.*, 2000, **172**, 43–72.

18 S.-T. Lin and S. I. Sandler, *Ind. Eng. Chem. Res*, 2002, **41**, 899–913.

19 T. Zhou, Z. Wang, Y. Ye, L. Chen, J. Xu and Z. Qi, *Ind. Eng. Chem. Res.*, 2012, **51**, 5559–5564.

20 Z. Lyu, T. Zhou, L. Chen, Y. Ye, K. Sundmacher and Z. Qi, *Chem. Eng. Sci.*, 2014, **115**, 186–194.

21 Z. Song, T. Zhou, J. Zhang, H. Cheng, L. Chen and Z. Qi, *Chem. Eng. Sci.*, 2015, **129**, 69–77.

22 Y. Chen, S. Zhou, Y. Wang and L. Li, *Fluid Phase Equilib.*, 2017, **451**, 12–24.

23 Z. Song, T. Zhou, Z. Qi and K. Sundmacher, *ACS Sustain. Chem. Eng.*, 2017, **5**, 3382–3389.

24 M. Z. M. Salleh, M. K. Hadj-Kali, H. F. Hizaddin and M. Ali Hashim, *Sep. Purif. Technol.*, 2018, **196**, 61–70.

25 M. K. Hadj-Kali, M. Althuluth, S. Mokraoui, I. Wazeer, E. Ali and D. Richon, *Chem. Eng. Commun.*, 2020, **207**, 1264–1277.

26 Z. Lei, J. Zhang, Q. Li and B. Chen, *Ind. Eng. Chem. Res.*, 2009, **48**, 2697–2704.

27 J. Wang, Z. Song, H. Cheng, L. Chen, L. Deng and Z. Qi, *ACS Sustain. Chem. Eng.*, 2018, **6**, 12025–12035.

28 Z. Song, C. Zhang, Z. Qi, T. Zhou and K. Sundmacher, *AIChE J.*, 2018, **64**, 1013–1025.

29 Z. Song, X. Li, H. Chao, F. Mo, T. Zhou, H. Cheng, L. Chen and Z. Qi, *Green Energy Environ.*, 2018, **4**, 154–165.

30 K. P. Paduszyński, M. Kroíikowski, M. Zawadzki and P. Orzeł, *ACS Sustain. Chem. Eng.*, 2017, **5**, 9032–9042.

31 Z. Lei, B. Chen and C. Li, *Chem. Eng. Sci.*, 2007, **62**, 3940–3950.

32 Z. Lei, C. Dai, X. Liu, L. Xiao and B. Chen, *Ind. Eng. Chem. Res.*, 2012, **51**, 12135–12144.

33 A. Fredenslund, R. L. Jones and J. M. Prausnitz, *AIChE J.*, 1975, **21**, 1086–1099.

34 M. Z. M. Salleh, M. K. Hadj-Kali, M. A. Hashim and S. Mulyono, *J. Mol. Liq.*, 2018, **266**, 51–61.

35 R. Anantharaj and T. Banerjee, *Ind. Eng. Chem. Res.*, 2010, **49**, 8705–8725.

36 J. A. Lazzús, *Fluid Phase Equilib.*, 2012, **313**, 1–6.

37 J. A. Lazzús and G. Pulgar-Villarroel, *J. Mol. Liq.*, 2015, **209**, 161–168.

38 C. Samorì, A. Pasteris, P. Galletti and E. Tagliavini, *Environ. Toxicol. Chem.*, 2007, **26**, 2379–2382.

39 A. Latała, M. Nędzi and P. Stepnowski, *Green Chem.*, 2009, **11**, 580–588.

40 D. Peng and F. Picchioni, *J. Hazard. Mater.*, 2020, **398**, 122964–122975.

41 R. Gani and K. M. Ng, *Comput. Chem. Eng.*, 2015, **81**, 70–79.

42 R. Gani and E. A. Brignole, *Fluid Phase Equilib.*, 1983, **13**, 331–340.

43 N. D. Austin, N. V. Sahinidis and D. W. Trahan, *Chem. Eng. Res. Des.*, 2016, **116**, 2–26.

44 P. Bonami, L. T. Biegler, A. R. Conn, G. Cornuéjols, I. E. Grossmann, C. D. Laird, J. Lee, A. Lodi, F. Margot, N. Sawaya and A. Wächter, *Discret. Optim.*, 2008, **5**, 186–204.

45 J. Currie, OPTI Toolbox, https://www.inverseproblem.co.nz/OPTI/index.php.

46 J. F. Tsai, M. H. Lin and Y. C. Hu, *Eur. J. Oper. Res.*, 2008, **184**, 802–809.

47 D. B. Hand, *J. Phys. Chem.*, 1930, **34**, 1961–2000.

48 D. Othmer and P. Tobias, *Ind. Eng. Chem.*, 1942, **34**, 693–696.

49 H. Renon and J. M. Prausnitz, *AIChE J.*, 1968, **14**, 135–144.

50 A. Marcilla, J. A. Reyes-Labarta and M. M. Olaya, *Fluid Phase Equilib.*, 2017, **433**, 243–252.

51 E. J. González, N. Calvar, B. González and A. Domínguez, *J. Chem. Eng. Data*, 2010, **55**, 4931–4936.

52 S. A. Sakal, C. Shen and C. X. Li, *J. Chem. Thermodyn.*, 2012, **49**, 81–86.

53 Z. Salleh, I. Wazeer, S. Mulyono, L. El-blidi, M. A. Hashim and M. K. Hadj-Kali, *J. Chem. Thermodyn.*, 2017, **104**, 33–44.

54 T. Zhou, Z. Wang, Y. Ye, L. Chen, J. Xu and Z. Qi, *Ind. Eng. Chem. Res.*, 2012, **51**, 5559–5564.

55 J. Chen, Z. Li and L. Duan, *J. Chem. Eng. Data*, 2000, **45**, 689–692.

56 T. Zhou, Z. Wang, L. Chen, Y. Ye, Z. Qi, H. Freund and K. Sundmacher, *J. Chem. Thermodyn.*, 2012, **48**, 145–149.

57 N. Calvar, I. Domínguez, E. Gómez and Á. Domínguez, *Chem. Eng. J.*, 2011, **175**, 213–221.

58 V. Štejfa, J. Rohlíček and C. Červinka, *J. Chem. Thermodyn.*, 2020, **142**, 106020–106029.

59 G. Annat, M. Forsyth and D. R. MacFarlane, *J. Phys. Chem. B*, 2012, **116**, 8251–8258.

60 M. G. Freire, A. R. R. Teles, M. A. A. Rocha, B. Schröder, C. M. S. S. Neves, P. J. Carvalho, D. V Evtuguin, L. M. N. B. F. Santos and J. A. P. Coutinho, *J. Chem. Eng. Data*, 2011, **56**, 4813–4822.

61 F. M. Gaciño, T. Regueira, L. Lugo, M. J. P. Comuñas and J. Fernández, *J. Chem. Eng. Data*, 2011, **56**, 4984–4999.

62 P. Wachter, C. Schreiner, H.-G. Schweiger and H. J. Gores, *J. Chem. Thermodyn.*, 2010, **42**, 900–903.

63 A. Ahosseini and A. M. Scurto, *Int. J. Thermophys.*, 2008, **29**, 1222–1243.

64 U. Domańska and M. Laskowska, *J. Solution Chem.*, 2008, **37**, 1271–1287.

65 K. R. Harris, M. Kanakubo and L. A. Woolf, *J. Chem. Eng. Data*, 2007, **52**, 2425–2430.

66 K. R. Harris, L. A. Woolf and M. Kanakubo, *J. Chem. Eng. Data*, 2005, **50**, 1777–1782.

67 C. P. Fredlake, J. M. Crosthwaite, D. G. Hert, S. N. V. K. Aki and J. F. Brennecke, *J. Chem. Eng. Data*, 2004, **49**, 954–964.

68 J. Zhang, S. Fang, L. Qu, Y. Jin, L. Yang and S. Hirano, *Ind. Eng. Chem. Res.*, 2014, **53**, 16633–16643.

69 M. Barycki, A. Sosnowska, A. Gajewicz, M. Bobrowski, D. Wileńska, P. Skurski, A. Giełdoń, C. Czaplewski, S. Uhl, E. Laux, T. Journot, L. Jeandupeux, H. Keppner and T. Puzyn, *Fluid Phase Equilib.*, 2016, **427**, 9–17.

70 S. Tang, G. A. Baker and H. Zhao, *Chem. Soc. Rev.*, 2012, **41**, 4030–4066.

71 A. Tot, M. Vraneš, I. Maksimović, M. Putnik-Delić, M. Daničić, S. Belić and S. Gadžurić, *Ecotoxicol. Environ. Saf.*, 2018, **147**, 401–406.

72 M. Królikowski, M. Królikowska, M. Więckowski and A. Piłowski, *J. Chem. Thermodyn.*, 2020, **147**, 9–14.